

Synthesis, spectroscopic characterization and computational studies of 2-(4-bromophenyl)-2-oxoethyl 3-methylbenzoate by density functional theory



Diwaker^a, C.S. Chidan Kumar^{b,c,*}, Ashish Kumar^a, Siddegowda Chandraju^d, Hoong-Kun Fun^{b,e}, Ching Kheng Quah^b

^aSchool of Basic Sciences, Indian Institute of Technology Mandi, Mandi, HP 175005, India

^bX-ray Crystallography Unit, School of Physics, Universiti Sains Malaysia (USM), 11800 Penang, Malaysia

^cDepartment of Engineering Chemistry, Alva's Institute of Engineering & Technology, Mijar, Moodbidri 57422, Karnataka, India

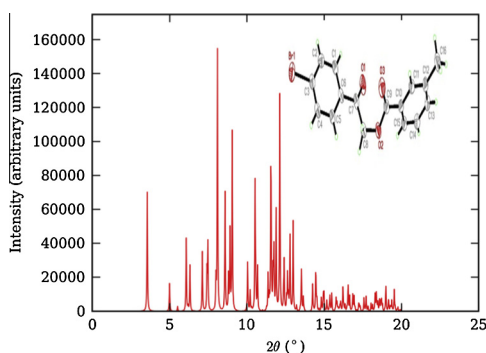
^dDepartment of Sugar Technology and Chemistry, Sir M. Visvesvaraya PG Center, University of Mysore, Tubinakere, Mandya 571402, India

^eDepartment of Pharmaceutical Chemistry, College of Pharmacy, King Saud University, Riyadh 11451, Saudi Arabia

HIGHLIGHTS

- Molecular structure of title compound is reported using DFT and X-ray analysis.
- NLO investigation reveals the title compound a strong candidate for SHG.
- IR and NMR spectra are computed using DFT approach.
- Band structure and TDOS along with PDOS are plotted.

GRAPHICAL ABSTRACT



ARTICLE INFO

Article history:

Received 13 December 2014

Received in revised form 13 March 2015

Accepted 17 March 2015

Available online 24 March 2015

Keywords:

DFT
DOS
GIAO
XRD
FTIR
NMR

ABSTRACT

The title compound, 2-(4-bromophenyl)-2-oxoethyl 3-methylbenzoate, has been synthesized and characterized using experimental FTIR, ¹H and ¹³C NMR, single crystal XRD and various theoretical methods (FTIR, NMR, electronic and band gap studies). The compound crystallizes in monoclinic space group *P*2₁/*c* with *a* = 8.176 (2) Å, *b* = 7.82 (2) Å, *c* = 2.952 (6) Å, β = 91.330 (4)° and *Z* = 4. The initial coordinate geometry obtained by XRD is further used to obtain the optimized ground state geometry of the investigated compound using HF and DFT/B3LYP/6-311++G(2d,2p) level of theory. Geometrical parameters, vibrational frequencies, (GIAO) ¹H and ¹³C NMR chemical shifts have been calculated theoretically using the optimized ground state geometry. Apart from this, density of states of different atoms, total density of states and band gap studies have also been successfully studied using theoretical models.

© 2015 Elsevier B.V. All rights reserved.

* Corresponding author at: Department of Engineering Chemistry, Alva's Institute of Engineering & Technology, Mijar, Moodbidri 57422, Karnataka, India. Tel.: +91 9980200463.

E-mail address: chidankumar@gmail.com (C.S. Chidan Kumar).

Introduction

There have been long-standing interests in photo-releasable protecting groups, for their applications in various multistep synthesis. Keto ester is a derivative of an acid which is formed by

the reaction between an acid and a phenacyl bromide. They are well-known as protecting groups for carboxylic acids in organic synthesis and biochemistry [1,2]. The ease of using these photosensitive blocking groups is, they can easily be cleaved under completely neutral or mild conditions [3] and therefore used for the identification of organic acids. These derivatives have immense applications in the field of synthetic chemistry [4] such as in the synthesis of imidazoles and oxazoles as well as benzoxazepine [5]. These are also useful in peptide synthesis. Keto esters, an important class of versatile intermediates, have been reported to show antitumor activity against Ehrlich cells and HeLa cells [6]. They also regulate the flowering times of some plants [7]. Recent studies have revealed that they also exhibit inhibitory activity against two isozymes of 11β -hydroxysteroid dehydrogenases (11β -HSD1 and 11β -HSD2), which catalyze the inter-conversion of active cortisol and inactive cortisone [8]. Many researchers have reported the synthesis and photolysis studies of phenacyl esters. Dicarboxyl compounds and their derivatives are also among the most versatile and frequently employed synthons in organic synthesis, especially in heterocyclic chemistry [9,10]. Hence phenacyl benzoates attract commercial importance due to their immense applications in various fields of chemistry. In continuation of our work [11–13], herewith we report the synthesis of 2-(4-bromophenyl)-2-oxoethyl 3-methylbenzoate, (1), which may be used as an effective synthon in synthetic chemistry.

Experimental and theoretical methods

Synthesis

The reagents and solvents for the synthesis were obtained from the Aldrich Chemical Co., and were used without additional purification. The title ester derivative was synthesized as per the procedure reported earlier [14–16]. 2-Bromo-1-(4-bromophenyl)ethan-1-one (0.01 mol) and *m*-toluic acid (0.015 mol) was dissolved in 8 ml dimethyl formamide. A slight excess of anhydrous potassium carbonate was added to the solution with vigorous stirring. The reaction mixture was stirred for about 2 h at room temperature. The progress of the reaction was monitored by TLC. The formed products were filtered and recrystallized. Crystals suitable for X-ray diffraction studies were obtained from acetone solution by slow evaporation technique at room temperature. Melting point (374–376 K) was determined by Stuart Scientific (UK) apparatus. The purity of the compound was confirmed by thin layer chromatography using Merck silica gel 60 F254 coated aluminum plates.

Solubility study

It is well-known that, solvent and temperature plays a significant role in growing the single crystals. The challenge is to select a suitable solvent for the slow evaporation crystal growth technique. In order to choose the best solvent, the solubility studies in various solvents are done and came to know that, the title compound is insoluble in water, less soluble in ethanol and methanol and moderately soluble in acetone and DMF. A known volume of the solvent is taken in a clean beaker and heated to a specific temperature. The finely powdered sample was added slowly to the solvent with stirring to get a saturated solution. About 20 ml of this saturated solution was transferred to a pre-weighed specific gravity bottle and weighed again. The difference in weight of the bottle containing the solution and the weight of the empty bottle gave the actual weight of the solution taken. The solution from the gravity bottle is transferred to a clean beaker, evaporated to dryness

and weighed to get the amount of solute present in the solution. The percentage solubility can be determined using the formula:

$$\text{Solubility (wt\%)} = \frac{(\text{weight of the solute} \times 100)}{\text{weight of the (solute + solvent)}}$$

This process was repeated thrice to get the accurate results at different temperatures in acetone and DMF and the solubility parameters were estimated. It is known that, the compound in which it is moderately soluble is chosen for crystal growth. The compound is very moderately soluble and steadily increases with both acetone and DMF. Since the slow evaporation of DMF takes considerably long duration, acetone was used to grow the single crystals of the title ester compound.

Crystal growth

To grow single crystals of the title ester derivative, the slow evaporation technique at constant temperature method was employed. A saturated solution of the compound in acetone as solvent was prepared and warmed slightly to get a homogeneous mixture. The solution was filtered to remove any impurities present and was kept undisturbed for few days. The mouth of the beaker was covered with filter paper to ensure slow evaporation. The defect free seed crystals obtained in this way were used for growing bulk crystals. The grown crystals are shown in Fig. 1.

Crystallography

Colorless, block shaped single crystal of the analyzed compound ($C_{16}H_{13}BrO_3$), with dimensions of 0.93 mm \times 0.54 mm \times 0.25 mm was selected and mounted on a Bruker APEX-II CCD diffractometer with a fine-focus sealed tube graphite-monochromated Mo $K\alpha$ radiation ($\lambda = 0.71073 \text{ \AA}$) at 296 K in the range of $2.5 \leq \theta \leq 23.9^\circ$. The data were processed with SAINT and corrected for absorption using SADABS [17]. A total of 16230 reflections were collected, of which 4257 were independent and 2660 reflections with $I > 2\sigma(I)$. The structures were solved by direct method using the program SHELXTL [18] and were refined by full-matrix least squares technique on F^2 using anisotropic displacement parameters for all non-hydrogen atoms. All the hydrogen atoms were positioned geometrically [$C-H = 0.93-96 \text{ \AA}$] and refined using riding model with isotropic displacement parameters set to 1.2 or 1.5

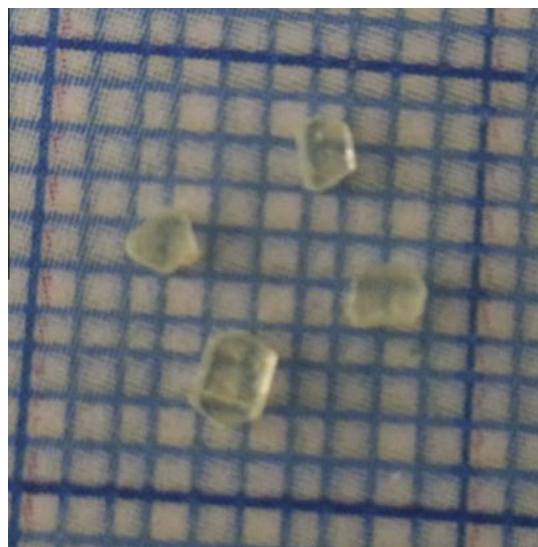


Fig. 1. Crystals grown by the slow evaporation technique.

Table 1
Crystal data and parameters for structure refinement of the title compound.

<i>Crystal data</i>	
Chemical formula	C ₁₆ H ₁₃ BrO ₃
<i>M_r</i>	333.17
Crystal system, space group	Monoclinic, <i>P</i> ₂ ₁ / <i>c</i>
Temperature (K)	296
<i>a</i> , <i>b</i> , <i>c</i> (Å)	8.176 (2), 7.82 (2), 2.952 (6)
β (°)	91.330 (4)
<i>V</i> (Å ³)	1468.6 (7)
<i>Z</i>	4
Radiation type	Mo K α
μ (mm ⁻¹)	2.80
Crystal size (mm)	0.93 × 0.54 × 0.25
<i>Data collection</i>	
Diffractometer	Bruker APEX-II CCD diffractometer
Absorption correction	Multi-scan (SADABS; Bruker, 2009)
<i>T_{min}</i> , <i>T_{max}</i>	0.181, 0.535
No. of measured, independent and observed [<i>I</i> > 2 σ (<i>I</i>)] reflections	16320, 4257, 2660
<i>R_{int}</i>	0.051
(<i>sin</i> θ / λ) _{max} (Å ⁻¹)	0.704
<i>Refinement</i>	
$R[F^2 > 2\sigma(F^2)]$, $wR(F^2)$, <i>S</i>	0.045, 0.125, 1.00
No. of reflections	4257
No. of parameters	181
H-atom treatment	H atoms treated by a mixture of independent and constrained refinement
$\Delta\rho_{max}$, $\Delta\rho_{min}$ (e Å ⁻³)	0.46, -0.58

(methyl group) times the equivalent isotropic *U* values of the parent carbon atoms. A rotating group model was used for methyl groups. The final full-matrix least squares refinement gave $R = 0.045$ and $wR = 0.125$ ($w = 1/[\sigma^2(F_o^2) + (0.0546 P)^2 + 0.3051 P]$ where $P = (F_o^2 + 2F_c^2)/3$, $S = 1.00$, $(\Delta/\sigma)_{max} = 0.004$, $\Delta\rho_{max} = 0.46$ e Å⁻³ and $\Delta\rho_{min} = -0.58$ e Å⁻³. A summary of crystal data and parameters for structure refinement details are given in Table 1.

Computational details

All theoretical calculations in the current work has been performed by using Gaussian 09 package along with CASTEP package. For simulation purpose the initial coordinates obtained from X-ray analysis are used in both the packages to obtain the optimized geometry of the title compound both at HF and DFT level of theory using 6-311++G(2d,2p) basis set [19–21]. The Vibrational frequency, chemical shifts, DOS and electronic band structures for title compound has been calculated using optimized geometries.

Results and discussions

Molecular geometry

The structure as analyzed from the X-ray analysis as well as from the optimized ground state geometry of the title compound are shown in Fig. 2. The compound with chemical formula, C₁₆H₁₃BrO₃, crystallizes in monoclinic system with space group *P*₂₁/*c* with unit cell dimensions $a = 8.176$ (2) Å, $b = 7.82$ (2) Å, $c = 2.952$ (6) Å and with the volume of 1468.6 (7) Å³. The Ortep diagram of 2-(4-bromophenyl)-2-oxoethyl 3-methylbenzoate, with atom labeling scheme drawn at 50% probability displacement ellipsoid is also depicted in Fig. 2. The molecular structure of the title compound consists of a bromophenyl ring and a substituted phenyl ring connected by a flexible C(=O)–O–C–C(=O) chain. The phenyl rings (C1–C6 and C10–C15) lie almost perpendicular to each other, with the dihedral angle between these two aromatic rings being 86.03 (12)°. In the structure, strong C–H...O hydrogen

bonds and Br...O short contacts dominates in the crystal packing. The C4–H4A...O1 (Symmetry code: $x, y - 1, z$) hydrogen bond connects the molecules into head-to-tail chains (Fig. 3a) propagating along the crystallographic *b*-axis direction. Two adjacent anti-parallel chains are interconnected via Br...O short contacts (3.301 Å) forming 2D supramolecular layer (Fig. 3b). Further, the crystal packing is stabilized by C–H... π (Table 2) interactions producing a three dimensional network involving the centroids of the C1–C6 and C10–C15 benzene rings. The bond length and bond angles agree with the literature values [22] and are comparable with those reported earlier. Simulated PXRD diagram for the title compound using *plotCIF* is depicted in Fig. 4. The title compound shows different types of bond interactions i.e. C–H...O. As seen from Table 2, atom C4 acts as a donor to the symmetry related at $x, y - 1, z$ [3.277 (3) Å]. Bond length and bond angle of such kind interactions are listed in Table 2. Using the initial coordinates obtained from the X-ray analysis, we have optimized the ground state geometry of the title compound using B3LYP/6-311++G(2d,2p) level of theory. The title compound possesses C1 point group, dipole moment of 2.11 Debye and ground state energy around -3417.62 atomic units. Some of the theoretically optimized parameters of the title compound which included bond length, angles and torsion angles are compared with experimental data and are given in Table 3. The correlation values of 0.9956 for bond lengths and 0.9928 for bond angles is obtained respectively.

The optimized parameters of title compound along with their experimental counterparts are given in Table 3.

The good correlation values obtained for both the bond length as well as bond angles suggests that the theoretical values obtained by DFT approach are in close agreement with their experimental counterparts. The difference in a few compared values may be due to the fact that, the experimental values correspond to solid phase, while the theoretical values corresponds to gas phase. The existence of crystal field along with intermolecular interactions connects the molecule together, which results in the difference between the compared parameters [23].

NMR spectra

NMR spectroscopy is considered to be a valuable and remarkable tool for structural and functional characterization of molecules. Theoretical GIAO ¹H and ¹³C NMR chemical shifts of the title compound with respect to TMS has been calculated using HF and DFT approach at B3LYP level of theory using 6-311++G(2d,2p) basis set. Solvents effect in the theoretical NMR has been included using CPCM model with chloroform available in g09 package. The experimental NMR for the title compound has been given in Figs. 5 and 6 respectively. The experimental ¹H NMR chemical shifts of the title compound may be read as ¹H NMR (500 MHz, CDCl₃): δ ppm 7.972 (s, 1H, methylbenzoate), 7.962–7.946 (d, 1H, *J* = 7.7 Hz), 7.869–7.852 (d, 2H, *J* = 8.5 Hz, Bromophenyl), 7.686–7.669 (d, 2H, *J* = 8.5 Hz, Bromophenyl), 7.444–7.429 (d, 1H, *J* = 7.7 Hz, methylbenzoate), 7.399–7.368 (t, 1H, *J* = 7.7 Hz, methylbenzoate) 5.537 (s, 2H, CH₂), 2.443 (s, 3H, CH₃). Theoretically the present compound under investigation, has 13 protons out of which eight protons are aromatic protons, two are aliphatic protons and three are attached to methyl group. Aliphatic protons shows a singlet peak at 6.01 ppm and 5.02 ppm using HF approach while 6.61 ppm and 5.52 ppm using DFT approach. The aromatic protons shows singlet peak in the range of 7.7–8.7 ppm using HF and in the range of 8.0–8.5 ppm using DFT approach. On comparison as shown in Table 4, we found that the investigated compound gave better chemical shifts with DFT approach than of HF approach and are near the experimental counterparts. The title compound also consists of 16 carbon atoms, out

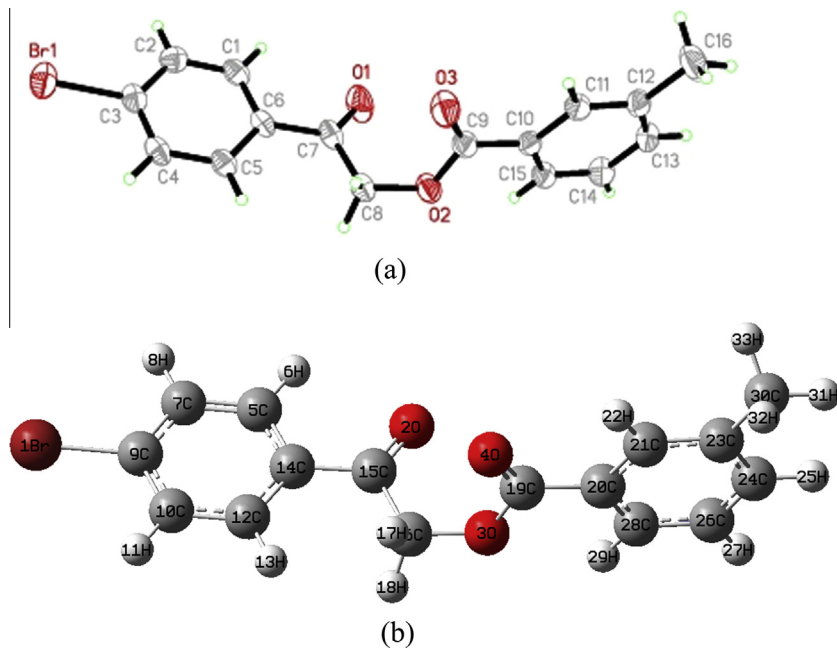


Fig. 2. (a) Displacement ellipsoids for title compound are drawn at 50% probability level. (b) Theoretical ground state structure of title compound at (B3LYP/6-311++G(2d,2p) level of theory.

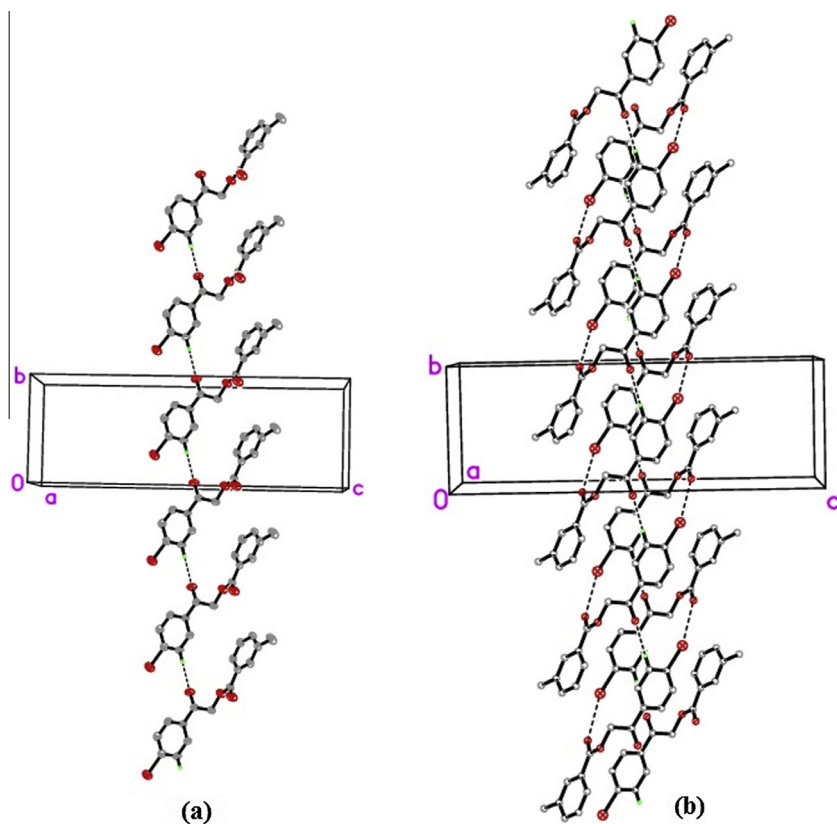


Fig. 3. Crystal packing of the title compound, showing intermolecular C–H...O hydrogen bonding interactions and Br...O short contacts as dotted lines. H atoms not involved in hydrogen bonding are omitted for clarity.

of which 13 atoms are aromatic carbon and the remaining are aliphatic carbon atoms. The aromatic carbon atoms shows singlet peak in the range of 121.72–165.20 ppm using HF approach and in the range of 133.96–173 ppm using DFT approach. The ^{13}C chemical shifts of the title compound are also observed

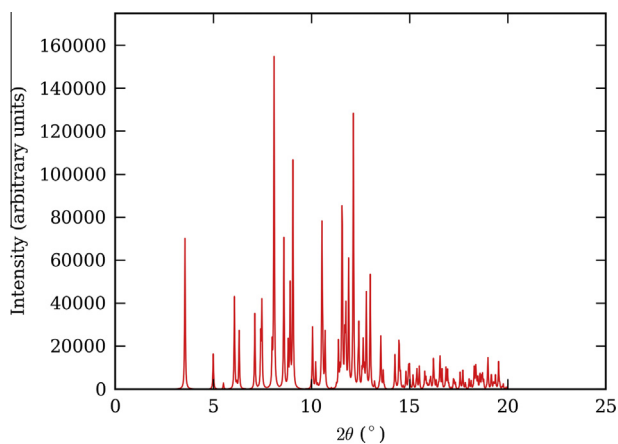
experimentally and can be read as ^{13}C NMR (125 MHz, CDCl_3): δ ppm 191.39 (C=O), 166.17 (O–C=O), 138.32, 134.24, 133.09, 132.27, 130.49, 129.34, 129.17, 129.14, 128.40, 127.14 (Ar), 66.24 (CH₂), 21.26 (CH₃) The calculated chemical shifts for the title compound are summarized in [Tables 5 and 6](#) respectively in detail.

Table 2
Hydrogen-bond geometry (Å, °).

<i>D</i> — <i>H</i> ··· <i>A</i>	<i>D</i> — <i>H</i>	<i>H</i> ··· <i>A</i>	<i>D</i> ··· <i>A</i>	<i>D</i> — <i>H</i> ··· <i>A</i>
C4—H4A···O1 ⁱ	0.93	2.36	3.277 (3)	170
C(13)—H(13A)···Cg(2) ⁱⁱ	0.93	2.92	3.770 (3)	153
C(15)—H(15A)···Cg(1) ⁱⁱⁱ	0.93	2.86	3.675 (3)	147

Symmetry codes:

- ⁱ *x*, *y* − 1, *z*.
ⁱⁱ −*x*, *y* + 1/2, −*z* + 3/2.
ⁱⁱⁱ −*x*, −*y* + 1, −*z* + 2.

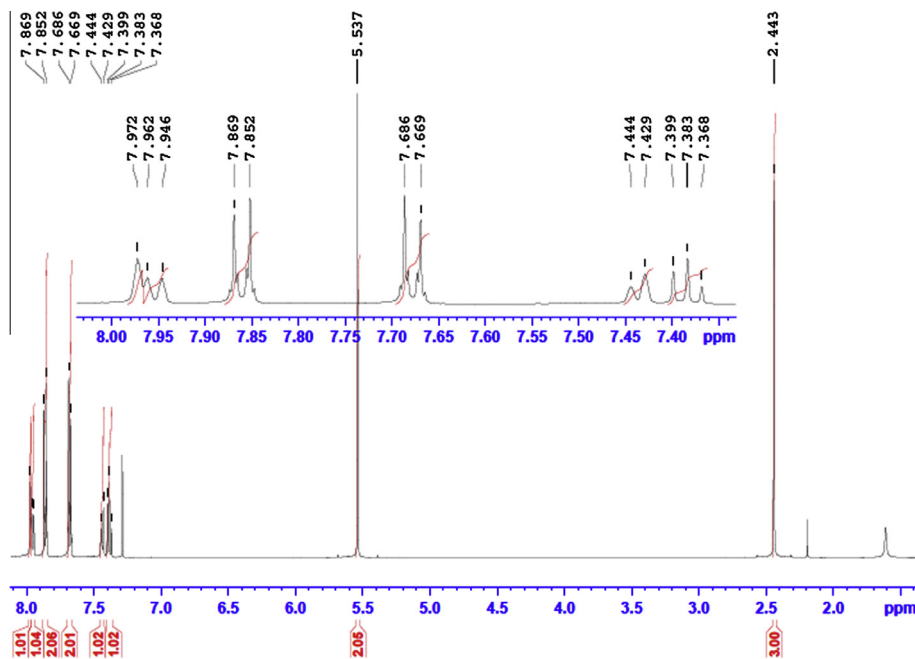
**Fig. 4.** Simulated PXRD diagram for the title compound using plotCIF.

IR spectra

In the present work, the IR spectra of the title compound has been computed theoretically using both HF and DFT approaches. The compound possesses C1 point group with 93 normal modes of vibrations and do not contain any imaginary frequency. The computed IR spectra of the title compound is shown in Fig. 7.

Table 3
Randomly selected geometrical parameters for title compound in (Å, °).

Numbering scheme (X-ray structure)	Experimental (X-ray)	Numbering scheme (DFT calculated structure)	DFT/6-311++(2d,2p)/B3LYP
Bond length			
Br1—C3	1.89	Br1—C9	1.90
O1—C7	1.20	O2—C15	1.20
O2—C9	1.34	O3—C19	1.35
O2—C8	1.43	O3—C16	1.41
O3—C9	1.20	O4—C19	1.20
C1—C2	1.37	C5—C7	1.38
C1—C6	1.39	C5—C14	1.39
C2—C3	1.39	C7—C9	1.39
C3—C4	1.37	C9—C10	1.38
C4—C5	1.38	C10—C12	1.38
C5—C6	1.39	C12—C14	1.39
C6—C7	1.49	C14—C15	1.49
C7—C8	1.50	C15—C16	1.51
C9—C10	1.48	C19—C20	1.48
C10—C15	1.38	C20—C28	1.39
C10—C11	1.39	C20—C21	1.39
C11—C12	1.38	C21—C23	1.39
C12—C13	1.39	C23—C24	1.39
C12—C16	1.51	C23—C30	1.51
C13—C14	1.37	C24—C26	1.38
C14—C15	1.37	C26—C28	1.38
Br1—C3	1.89	Br1—C9	1.90
O1—C7	1.20	O2—C15	1.20
O2—C9	1.34	O3—C19	1.35
O2—C8	1.43	O3—C16	1.41
O3—C9	1.20	O4—C19	1.20
C1—C2	1.37	C5—C7	1.38
C1—C6	1.39	C5—C14	1.39
Bond angles			
C9—O2—C8	114.83	C19—O3—C18	115.83
C4—C3—Br1	119.38	C10—C9—Br1	119.29
C2—C3—Br1	119.20	C7—C9—Br1	119.41
O1—C7—C6	121.30	O2—C15—C14	121.74
O1—C7—C8	120.50	O2—C15—C16	120.60
O2—C8—C7	111.0	O3—C16—C15	111.0
O3—C9—O2	123.10	O4—C19—O3	123.60
O3—C9—C10	124.8	O4—C19—C20	124.9
O2—C9—C10	112.10	O3—C19—C20	112.30

**Fig. 5.** Experimental ¹H NMR chemical shifts of the title compound.

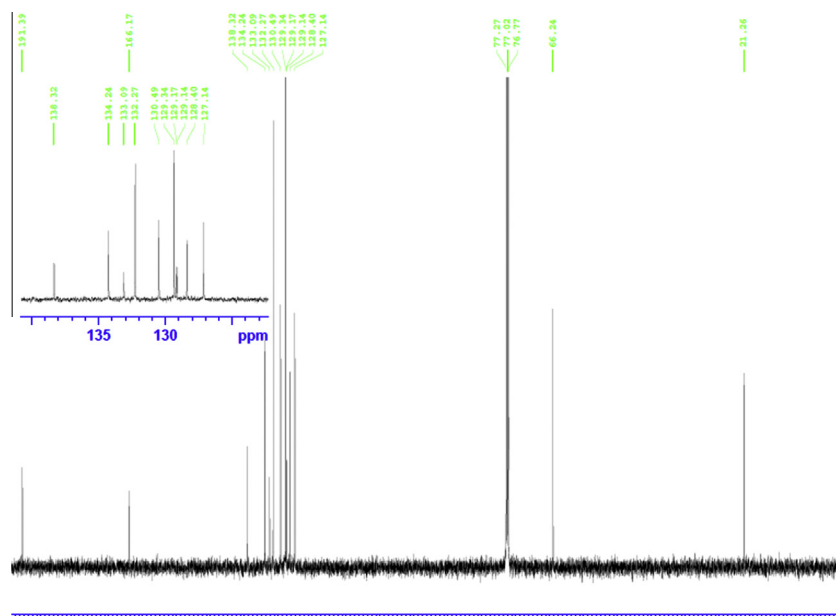


Fig. 6. Experimental ^{13}C NMR chemical shifts of the title compound.

Table 4

^1H NMR chemical shifts(ppm) relative to the TMS for the title compound using B3LYP/6-311++G(2d,2p) level of theory.

Atoms	Aromatic/aliphatic	HF/B3LYP/6-311++G(2D,2P)	DFT/B3LYP/6-311++G(2D,2P)	Experimental
H6	Ar CH	8.8	8.57	7.80
H8	Ar CH	7.8	8.11	7.67
H11	Ar CH	7.91	8.03	7.67
H13	Ar CH	8.37	8.38	7.80
H17	CH	6.01	6.61	5.53
H18	CH	5.02	5.52	5.53
H22	Ar CH	8.73	8.38	7.97
H25	Ar CH	8.04	8.05	7.44
H27	Ar CH	7.73	7.89	7.37
H29	Ar CH	8.55	8.56	7.95
H31	CH_3	2.17	2.32	2.44
H32	CH_3	2.54	2.79	2.44
H33	CH_3	2.53	2.76	2.44

Table 5

^{13}C NMR chemical shifts (ppm) relative to the TMS for the title compound using B3LYP/6-311++G(2d,2p) level of theory.

Atoms	Aromatic/aliphatic	HF/B3LYP/6-311++G(2D,2P)	DFT/B3LYP/6-311++G(2D,2P)	Experimental
C5	Ar C	127.9	133.8	130.4
C7	Ar C	125.6	136.7	132.7
C9	Ar C	140.5	154.0	128.4
C10	Ar C	125.2	136.3	132.2
C12	Ar C	127.2	134.6	130.4
C14	Ar C	125.5	136.8	134.2
C15	C	190.4	199.8	191.0
C16	CH	52.6	69.5	66.2
C19	Ar C	165.2	173.0	166.1
C20	Ar C	121.7	133.9	129.1
C21	Ar C	129.9	136.5	129.3
C23	Ar C	133.8	146.4	138.3
C24	Ar C	132.5	136.8	133.0
C26	Ar C	121.9	132.8	129.1
C28	Ar C	124.5	131.2	127.1
C30	CH_3	8.6	21.4	21.2

Table 6

Assignment of selected modes of vibration for the title compound.

S. No.	Modes of vibration	Calculated		Experimental
		HF/B3LYP/6-311++G(2d,2p)	DFT/B3LYP/6-311++G(2d,2p)	
1	$\nu\text{C}-\text{H}_{\text{aromatic}}$	3263	3296	2944
2	$\Gamma\text{C}-\text{H}_{\text{aromatic}}$	1096	1085	1068
3	$\nu\text{C}-\text{Br} + \Gamma\text{C}=\text{O}$	523	685	685
4	$\Gamma\text{C}-\text{Br}$	194	197	200
5	$\nu\text{C}=\text{O}$	1824	1768	1722
6	$\nu\text{C}-\text{O}$	1291	1385	1396
7	νCCH_3	3107	3109	3089
s8	$\nu\text{C}=\text{Cring1}$	1526	1623	1609
9	$\nu\text{C}=\text{Cring2}$	1637	1643	1698

Vibrational modes: ν , stretching, Γ , Bending, abbreviations: s, symmetric, ring 1 (C5–C7–C9–C10–C12–C14), ring 2 (C20–C21–C23–C24–C26–C28).

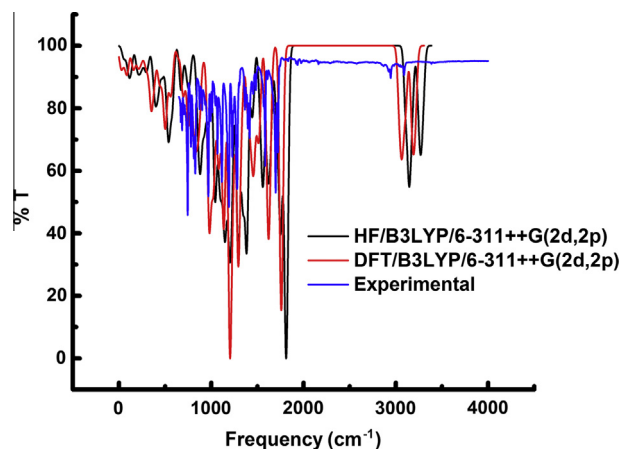


Fig. 7. Simulated [HF/DFT/B3LYP/6-311++g(2d,2p) levels] FT-IR spectra of the title compound.

Table 7

Calculated polarisability (α) and first hyperpolarisability (β) using DFT/B3LYP/6-311++G(2d,2p) level of theory in atomic units (a.u) for our title compound.

DFT/B3LYP/6-311++G(2d,2p)	
α_{xx}	10.47
α_{xy}	-0.15
α_{yy}	-6.14
α_{xz}	-1.93
α_{yz}	3.04
α_{zz}	-4.32
α_{tot}	15.16
β_{xxx}	-13.86
β_{xxy}	16.60
β_{xyy}	36.25
β_{yyy}	0.94
β_{xxz}	26.33
β_{xyz}	5.05
β_{yyz}	2.6
β_{xzz}	96.24
β_{yzz}	4.56
β_{zzz}	-7.24
β_{tot}	122.60

The experimental IR spectra of the title compound is also given in Fig. 8. The vibrational bands have been assigned using Gauss View molecular visualization program and calculated bands with both HF and DFT approach along with selected experimental counterparts are presented in Table 6.

Aromatic C–H vibrations

The bands in the region 3100–3000 cm^{-1} are due to CH stretching vibrations in aromatic compounds [24,25]. In the title compound, the bands observed in the IR spectra and with the help of Gauss View Molecular visualization program are in the range of 3146–3185 cm^{-1} are assigned to CH stretching vibrations of aromatic rings at HF level of theory. Along with this, out of plane bending vibrations of aromatic ring is also observed at 965, 988 and 1096 cm^{-1} respectively. Using DFT approach the bands observed in the range 3166–3196 cm^{-1} are assigned to CH stretching vibrations, while the bands observed at 977, 957 and 1085 cm^{-1} respectively are assigned to the out of plane bending vibrations of aromatic rings.

C–Br vibrations

According to literature values, the bending C–Br vibrations generally occurs in the range of 100–400 cm^{-1} and C–Br stretching vibrations ranging 690–515 cm^{-1} [26]. We have investigated such kind of vibrations in the present compound using both HF and DFT approach. Using HF approach we found that the bands observed at 194 cm^{-1} are assigned to C–Br bending vibrations and that at 523 cm^{-1} are assigned to C–Br stretching vibrations. The bending mode is a pure mode while stretching mode is mixed with C=O bending vibrations. Using DFT approach we found that the band assigned at 685 cm^{-1} correspond to C–Br stretching modes which is mixed with C=O bending modes of vibrations while the one observed at 197 cm^{-1} is a pure mode and is for C–Br bending modes of vibrations.

C=O vibrations

C=O stretching vibrations generally occurs in the range of 1670–1820 cm^{-1} . Using HF approach the bands at 1526, 1703, 1806 and 1824 cm^{-1} are assigned to C=O stretching vibrations. Out of these bands, the one at 1824 cm^{-1} is highly intense and a pure band. The bands at 1600, 1755 and 1768 cm^{-1} are assigned to C=O stretching vibrations using DFT approach among which, the band at 1768 cm^{-1} is intense in comparison to other observed bands.

C–O vibrations

C–O stretching vibrations generally occurs in the range 1000–1320 cm^{-1} as reported in literature. The bands observed at 1040, 1115, 1117, 1180, 1199, 1222, 1291, 1385 cm^{-1} respectively are assigned to C–O stretching vibrations using HF approach. Out of all these bands, the one observed at 1040 cm^{-1} is a pure mode while other modes of vibrations is mixed with C=C stretching and bending modes of vibrations. The bands observed at 1080, 1115, 1115, 1222, 1199, 1291, 1385 cm^{-1} respectively are observed using DFT approach and shows a similar trend of pure and impure modes as calculated using HF approach, while the one observed at 1385 cm^{-1} is an intense band.

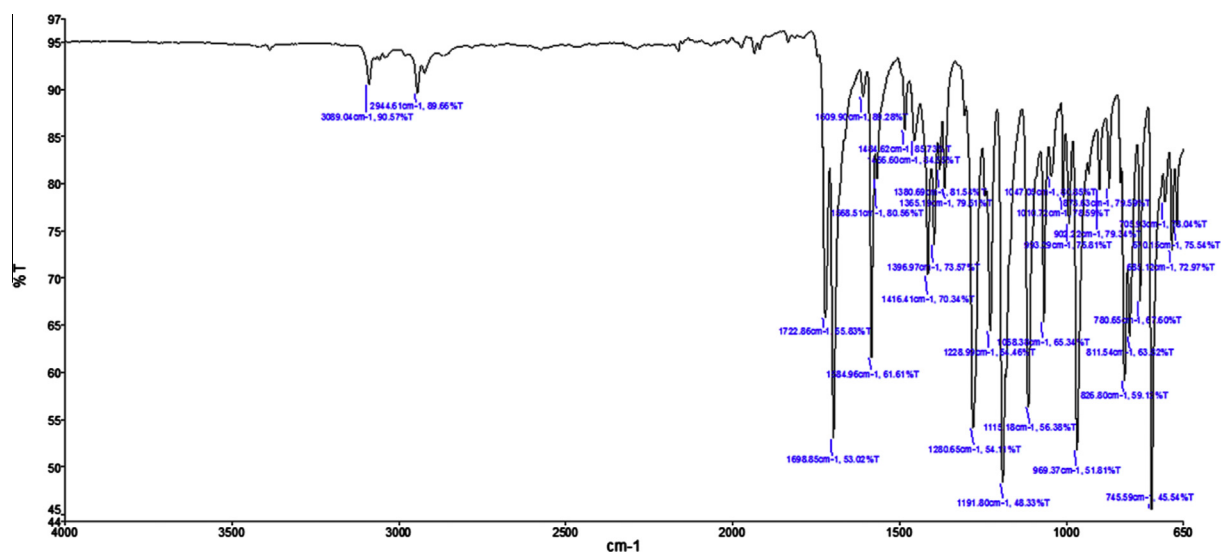


Fig. 8. Experimental IR spectra of title compound.

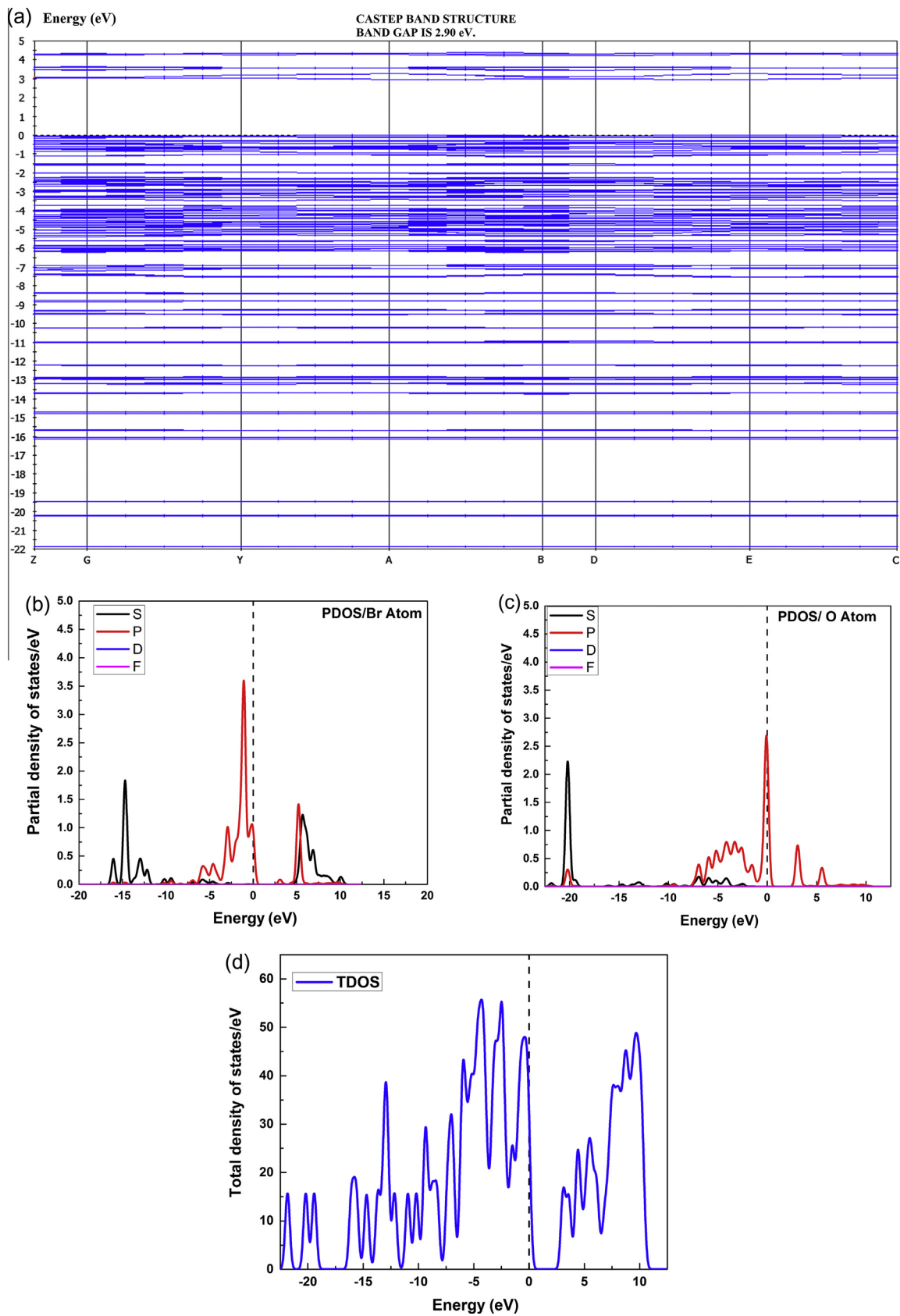


Fig. 9. Band gap, TDOS and PDOS of title compound.

C=C vibrations

As per the literature reports, the available C=C stretching vibrations generally occurs in the range (1400–1600) cm^{-1} . In the title compound there are C=C stretching vibrations in two rings namely ring 1 (C5–C7–C9–C10–C12–C14) and ring 2 (C20–C21–C23–C24–C26–C28). The bands observed using HF approach at 1526 cm^{-1} are due to C=C stretching vibrations of ring 1, while the bands observed at 1554, 1565, 1637 cm^{-1} respectively are due to C=C stretching vibrations of ring 2. Similarly using the DFT approach, the bands observed at 1504 and 1643 cm^{-1} are assigned to C=C stretching vibrations of ring 2, while the bands observed at 1523, 1600, 1623, 1622 cm^{-1} respectively are assigned to C=C stretching vibrations of ring 1.

CH₃ vibrations

Methyl vibrations are generally occur in the range (2900–3000) cm^{-1} . The bands observed in the range (3000–3185) cm^{-1} using HF are assigned to different modes of methyl vibrations which varies from stretching, bending, twisting modes of vibrations. Using DFT approach the bands observed at 3109 cm^{-1} and 3111 cm^{-1} are assigned to stretching methyl vibrations.

Non-linear optical (NLO) effects

Type of molecules which shows asymmetric polarization induced due to electron donor and acceptor groups in pi-electron conjugated systems are potential candidates for electro optic and NLO applications [27,28]. The investigated compound was subjected for such kind of possible applications by theoretical approach using Gaussian package. Our study includes the calculation of first hyperpolarisability tensor for all 10 derivatives. First hyperpolarisability is a third rank tensor which is described by a $3 \times 3 \times 3$ matrix. The 27 components of this 3D matrix can be reduced to 10 components due to Kleinman symmetry [29]. The output from Gaussian provides ten components of its matrix as $\beta_{xxx}, \beta_{xxy}, \beta_{xyy}, \beta_{yyy}, \beta_{xxz}, \beta_{xyz}, \beta_{yyz}, \beta_{xzz}, \beta_{yzz}, \beta_{zzz}$ respectively. The calculations of mean polarisability (α_{tot}) and first hyperpolarisability (β_{tot}) in atomic units has been reported in the present work. The components of β can be calculated by using the following equation given below.

$$\beta_i = \beta_{iii} + \frac{1}{3} \sum_{i \neq j} (\beta_{ijj} + \beta_{jij} + \beta_{jji})$$

further using the x, y and z components of β , the magnitude of first hyperpolarisability can be calculated using the relation given as

$$\beta_{tot} = (\beta_x^2 + \beta_y^2 + \beta_z^2)^{1/2}$$

further the complete equation for calculating the magnitude of β_{tot} from package output is given as

$$\beta_{tot} = \left[(\beta_{xxx} + \beta_{xyy} + \beta_{xzz})^2 + (\beta_{yyy} + \beta_{yzz} + \beta_{yxx})^2 + (\beta_{zzz} + \beta_{zxx} + \beta_{zyy})^2 \right]^{1/2}$$

The values of polarisability (α_{tot}) and first hyperpolarisability (β_{tot}) calculated using DFT approach along with B3LYP functional and 6-311++G(2d,2p) basis set for the title compound are summarized in Table 7.

The calculated values of polarisability (α_{tot}) and first hyperpolarisability (β_{tot}) comes out to be as 15.16 a.u and 122.60 a.u. The threshold values for NLO effects is that of Urea used for comparison purposes whose polarisability and first

hyperpolarisability values are 15.56 a.u and 59.4 a.u. respectively. Since from the computed results, the values are 1 and 2 times that of standard values. So we propose that the compound under investigation is a strong potential material for NLO applications like frequency doubling and SHG.

Band structure, PDOS and TDOS

Density of states (partial and total) along with band structure of a material or a particular type of compound is useful in predicting the physical properties such as electrical resistivity, optical absorption and to understand the solid state device physics. We have reported the band structure, partial and total density of states using GGA approximation with ultrasoft pseudopotentials in reciprocal space. The computed TDOS, PDOS and band structure of the title compound are shown in Fig. 9a–d. The computed energy gap using GGA approximation along with PBE functional comes out to be 2.960 eV. In the title compound, it has bromine and oxygen atoms apart from carbon and hydrogen which contributes to the density of states. The total density of states along with partial density of states are plotted in Fig. 9b–d. Partial density of states gives information about the contribution of individual states for formation of band gaps. From Fig. 8b (PDOS for bromine atom) it is found that, in the energy range –22 eV–10 eV, s-states of bromine atom contributes to the band formation while near the fermi level the contribution from p states is more. A similar trend is observed in the energy range from 5 eV to 10 eV with negligible contribution from the d and f states of bromine atom. In case of oxygen atom, it has more contribution from s-states near energy 20 eV while near the fermi level p-states are dominant over all other states with negligible contribution from d and f states of oxygen atom. The total density of states for the title compound is depicted in Fig. 9d.

Conclusion

In conclusion, a novel ester compound which could be a potential synthon in synthetic chemistry has been synthesized. The structure of the compound has been determined by both X-ray analysis as well as DFT approach. Molecular geometry obtained using DFT approach shows an excellent agreement with that obtained with X-ray analysis. Various theoretical spectroscopic characterization like NMR and IR spectroscopy for optimized molecular structure of title compound has been done. NLO investigation reveals title compound a strong candidate for frequency doubling and SHG. Large band gap of around 2.90 eV make title compound suitable for many solid state device applications. TDOS and PDOS plots using GGA approximation along with PBE functional helps us in understanding the contribution of different states for band gap formation.

Acknowledgements

Diwaker would like to thank IIT Mandi for HTRA scholarship as well as computational facilities. C.S.C.K. thanks Universiti Sains Malaysia (USM) for a postdoctoral research fellowship (2013–2015). C.S.C.K., C.K.Q. & H.K.F. thank to USM for RUI 2014 Grant (No. 1001/PFIZIK/811278). The authors extend their appreciation to The Deanship of Scientific Research at King Saud University for the research group project no. RGP VPP-207.

References

- [1] J.B. Rafter, E. Reid, J. Am. Chem. Soc. 41 (1919) 75–83.
- [2] J.K. Litera, A.D. Loya, P. Klan, J. Org. Chem. 71 (2006) 713–723.
- [3] J.C. Sheehan, K. Umezaw, J. Org. Chem. 38 (1973) 3771–3773.

- [4] W. Huang, J. Pian, B. Chen, W. Pei, X. Ye, *Tetrahedron* 52 (1996) 10131–10136.
- [5] S.S. Gandhi, K.L. Bell, M.S. Gibson, *Tetrahedron* 51 (1995) 13301–13308.
- [6] M. Kinoshita, S. Umezawa, *S. Bull. Chem. Soc. Jpn.* 33 (1960) 1075–1080.
- [7] K. Kai, F. Yano, F. Suzuki, H. Kitagawa, M. Suzuki, M. Yokoyama, N. Watanabe, *Tetrahedron* 63 (2007) 10630–10636.
- [8] L. Zhang, Y. Shen, H.J. Zhu, F. Wang, Y. Leng, J.K. Liu, *J. Antibiot.* 62 (2009) 239–242.
- [9] H. Sheibani, M.R. Islami, A. Hassanpour, K. Saidi, *Phosphorus, Sulfur Silicon Relat. Elem.* 183 (2007) 13–20.
- [10] S. Pal, J. Mareddy, N.S. Devi, *J. Braz. Chem. Soc.* 19 (2008) 1207–1214.
- [11] C.S. Chidan Kumar, T.S. Chia, S. Chandraju, C.W. Ooi, C.K. Quah, H.K. Fun, *Zeitschrift für Kristallographie – Crystalline Materials* 229 (4) (2014) 328–342.
- [12] C.S. Chidan Kumar, C.Y. Panicker, H.-K. Fun, Y. Sheena Mary, B. Harikumar, S. Chandraju, C.K. Quah, C.W. Ooi, *Spectrochim. Acta Part A Mol. Biomol. Spectrosc.* 126C (2014) 208–219.
- [13] C.S. Chidan Kumar, H.K. Fun, M. Tursun, C.W. Ooi, S. Chandraju, C.K. Quah, C. Parlak, *Spectrochim. Acta Part A Mol. Biomol. Spectrosc.* 124C (2014) 595–602.
- [14] C.S.C. Kumar, T.S. Chia, S. Chandraju, C.W. Ooi, C.K. Quah, H.K. Fun, *Zeitschrift für Kristallographie – Crystalline Materials* 229 (4) (2014) 328–342.
- [15] C.S.C. Kumar, H.K. Fun, M. Tursun, C.W. Ooi, S. Chandraju, C.K. Quah, C. Parlak, *Spectrochim. Acta Part A Mol. Biomol. Spectrosc.* 124C (2014) 595–602.
- [16] C.S.C. Kumar, C.Y. Panicker, H.-K. Fun, Y. Sheena Mary, B. Harikumar, S. Chandraju, C.K. Quah, C.W. Ooi, *Spectrochim. Acta Part A Mol. Biomol. Spectrosc.* 126C (2014) 208–219.
- [17] Bruker, APEX2, SAINT and SADABS, Bruker AXS Inc., Madison, Wisconsin, USA, 2009.
- [18] G.M. Sheldrick, *Acta Cryst. A* 64 (2008) 112–122.
- [19] Diwaker, *Spectrochim. Acta Part A Mol. Biomol. Spectrosc.* 136C (2015) 1932–1940.
- [20] Diwaker, *Spectrochim. Acta Part A Mol. Biomol. Spectrosc.* 128 (2014) 819–829.
- [21] Diwaker, A.K. Gupta, *Int. J. Spectrosc.* 2014 (2014) 15. Article ID 841593.
- [22] F.H. Allen, O. Kennard, D.G. Watson, L. Brammer, A.G. Orpen, R. Taylor, *R. J. Chem. Soc. Perkin Trans. 2* (1987) S1–S19.
- [23] E. Inkaya, M. Dincer, *J. Mol. Struct.* 1026 (2012) 117–126.
- [24] G. Socrates, *Infrared characteristic group frequencies*, Wiley Interscience Publications, New York, 1980.
- [25] G. Varsanyi, *Vibrational Spectra of Benzene Derivatives*, Academic Press, New York, 1969.
- [26] A.A. Popov, V.M. Senyavin, A.A. Ganovsky, *Chem. Phys. Lett.* 383 (2004) 149–155.
- [27] I. Khan, A. Ahmad, *J. Phys. Chem. Solids* 74 (2013) 181.
- [28] J. Zyss, *Curr. Opin. Solid state Mater. Sci.* 1 (1996) 533.
- [29] D.A. Kleinman, *Phys. Rev.* 126 (1962) 1977.